Size effects on static and dynamic properties of ferroelectric nanoparticles

Th. Michael* and S. Trimper†
Institute of Physics, Martin-Luther-University, D-06099 Halle, Germany

J. M. Wesselinowa‡
Department of Physics, University of Sofia, Boulevard J. Bouchier 5, 1164 Sofia, Bulgaria
(Received 8 May 2007; revised manuscript received 3 July 2007; published 12 September 2007)

Ferroelectric nanoparticles are described by a microscopic model which enables one to find the macroscopic polarization as well as the excitation energy of the soft mode and its damping with dependence on the temperature and the size of the particles. The constituents of the material are arranged in shells, and their interaction depends on both the coupling at the surface and within the bulk. A Green's function technique in real space is applied to analyze the Ising model in a transverse field, which is modified in such a manner as to be able to study also spherical nanoparticles. Furthermore, we investigate the influence of size effects on the critical temperature. Whereas the excitation energy is lowered significantly with decreasing particle size, the damping is enhanced. Additionally, we consider the influence of defects on the excitation spectrum. The theoretical results are compared with experimental data.

DOI: 10.1103/PhysRevB.76.094107 PACS number(s): 77.80.−e, 61.46.Df, 77.80.Bh, 65.80.+n

I. INTRODUCTION

Although the influence of surface and size effects on phase transitions in ferroelectrics has been known since the 1950s,[1,2] there is a renewed and distinct interest in studying such effects. One reason for that is due to the great progress in the preparation of ferroelectric (FE) thin films and small FE particles as well as a broad variety of practical applications.[3] The experimental effort was closely connected with a theoretical modeling. Apart from the analytical approaches we are interested in, first-principles techniques play a decisive role in finding out the different dielectric properties of small FE particles or thin films. In particular, such *ab initio* methods have been improved since the 1990s, even for analyzing ferroelectric properties (for a recent review, cf. Ref. 4). Nowadays, a common method is the density functional theory (DFT).[5] The application of DFT to ferroelectric oxide nanostructures is also reported in Ref. 4. Due to the limitation of the number of atoms and the restriction at zero temperature, a microscopic effective Hamiltonian approach[6] was applied. The generalization for describing ferroelectricity was given by Zhong *et al.*[7] The involved parameters in that expansion are calculated via linear-response theory and the total energy within DFT. Other approaches are shell-model calculations[8] or a phenomenological model to simulate $Pb(Zr,Tr)O_3$ structures by chemical rules from DFT.[9] Recently, the ground-state polarization of $BaTiO_3$ (BTO) nanosized films and cells is studied using an atomic-level simulation approach on a shell model with parameters obtained from first-principles calculations.[10]

Whereas the application of analytical and *ab initio* methods, respectively, is mainly focused on a microscopic understanding of the ferroelectric nanomaterial, the former studies have been directed at the macroscopic properties like the shift of the phase transition temperature as a function of the size and at the existence of a critical particle size.[1,2,11–19] The experiments have been performed by applying x-ray and electron diffraction, specific heat measurements, and Raman scattering on particles of various sizes (see Ref. 17). Otherwise, the macroscopic behavior is directly triggered by the microscopic quantities such as the elementary excitations and their damping. Thus, evidence for the occurrence of a soft-mode behavior has been given by Refs. 16 and 17. Using x-ray or Raman-scattering methods in $PbTiO_3$ (PTO) fine particles, a soft-mode behavior was detected, designated as $E(1TO)$, which is shifted toward a low-frequency region with decreasing temperature. The damping associated with the excitations of, e.g., $SrBi_2Ta_2O_9$ (SBT)[20] or BTO[21] nanoparticles of various sizes increases with decreasing particle sizes. Further, the lattice vibration of smaller particles becomes softer than that of larger ones, because the soft-mode frequency at an arbitrary temperature decreases as the size decreases. In addition, this result implies a lowering of T_c with the shrinking of the particles. Diverse experiments report the existence of a critical size, which is still discussed controversially.[14,15] Referring to this, smaller particles offer no ferroelectric hysteresis loop or peak in the dielectric constant. The occurrence of vacancies, dislocation, and defects in nanoparticles has a strong influence on the static and dynamic properties; for a study of the dielectric properties of Fe-ion-doped BTO nanoparticles, see Ref. 22.

Concerning the analytical access to the description of ferroelectricity, the Landau-type phenomenological theories are still successful. By applying a Landau theory, the extrapolation length of a FE particle should be size dependent.[23,24] The influence of the size on the dielectric behavior of thin films, cylinders, and spheres is discussed in Refs. 25 and 26, where a size-driven phase transition in thin films was found. A study of the surface polarization enhancement and switching properties of small FE particles by using a time dependent Ginzburg-Landau model is given in Ref. 27. The influence of size effects and depolarization fields on the phase diagram of cylindrical FE nanoparticles is discussed in Ref. 28 using a variational method. Conservation and enhancement of FE properties in nanorods and nanowires are predicted.

The Ising model in a transverse field (TIM) is a promising candidate to figure out ferroelectric properties based on a microscopic Hamiltonian. Although the application of the TIM is mainly limited to ferroelectrics of order-disorder type, it has been used to find the size dependence of the mean polarization, the Curie temperature, and the susceptibility.[29–31] Recently, the Ising model in a transverse field was applied successfully to obtain the hysteresis of spherical ferroelectric particles.[32] The influence of size and doping as well as surface effects on the ferroelectric loop and the critical temperature was shown. In the majority of theoretical investigations, the influence of size effects on the mean polarization, the phase transition temperature T_c, and the susceptibility has been considered. On the other hand, the underlying dynamical properties, such as elementary excitations and damping effects, are not discussed adequately until now. Therefore, it is the purpose of the present paper to study the dynamical properties of FE particles and to discuss the influence of size effects on thermodynamic quantities. The analysis is based on the TIM, which is treated with the method of real-space Green's functions.

II. MODEL AND THE GREEN'S FUNCTION

In this section, we present the calculation scheme to get the Green's function for a spherical ferroelectric nanoparticle. The systems under consideration are often characterized by locally ordered regimes instead of a global long-range order. Our study is based on TIM, which is one of the basic models to analyze ferroelectric materials of the order-disorder type (see Ref. 33). To some extent, it can also be used for displacive type ferroelectrics.[34] The position of the hydrogen atom within a double well potential is mapped to an Ising spin, whereas the tunneling between both minima is described by the x-component of the spin. The double well structure is evaluated convincingly by using *ab initio* studies.[35,36] For an experimental observation of the momentum distribution of hydrogen in potassium dihydrogen phosphate (KDP), see Ref. 37. Due to the formulation of the model in terms of spin operators, we can apply the powerful technique available also for magnetic materials. Here, the ferroelectric constituents are characterized by spin operators, which should not be confused with the real spin of the material. Hence, these operators should be denoted as pseudospin operators. In the present paper, the dynamic properties of a spherical nanoparticle (see Fig. 1 and also Ref. 32) will be presented. The shells are numbered by $n=0, 1, \ldots, N$, where $n=0$ denotes the central spin and $n=N$ represents the surface shell of the system.

In this paper, we include actually bulk and surface properties by specifying the model parameters. For more refined results, these parameters should be calculated directly by first-principles calculations. The Hamiltonian of the TIM is given by

$$H = -\frac{1}{2}\sum_{ij} J_{ij} S_i^z S_j^z - \sum_i \Omega_i S_i^x, \tag{1}$$

where S_i^x and S_j^z are components of a spin-$\frac{1}{2}$ operator. The sums are taken over the internal and surface lattice points,

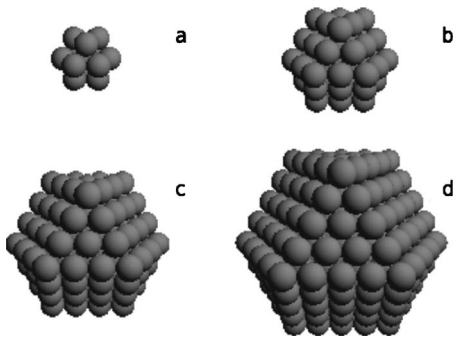

FIG. 1. Array of the ferroelectric nanoparticles composed of different shells. Each sphere represents a pseudospin situated in the center, where (a) consists of one central spin plus $N=1$ shell, (b) $N=2$, (c) $N=3$, and (d) $N=4$.

respectively. J_{ij} is an exchange interaction between spins at nearest neighbor sites i and j. For the inclusion of surface and doping effects into the model and the appropriate rotation of spin operators, see Ref. 32.

Macroscopic and microscopic quantities can be calculated by using the retarded Green's function, which is defined as

$$G_{lm}(t) = \langle\langle S_l^+(t); S_m^-(0)\rangle\rangle. \tag{2}$$

The operators S_l^+, S_m^- are the Pauli operators in the rotated system. Using the method introduced in Ref. 38 and modifying it for the real space, we obtain the excitation energy, occasionally denoted as pseudo-spin-wave energy. In the generalized Hartree-Fock approximation, the equation of motion reads

$$A_{lj} G_{jm} = 2\langle S_l^z\rangle \delta_{lm},$$

with the matrix

$$A_{lj} = \left\{ \hbar\omega - 2\Omega \sin\theta_l - \sum_i J_{li} \left[\cos\theta_i \cos\theta_l \langle S_i^z\rangle + \frac{1}{2}\sin\theta_l \sin\theta_i (\langle S_i^- S_l^-\rangle + \langle S_i^+ S_l^-\rangle) \right] \delta_{lj} + J_{jl} \left[\cos\theta_j \cos\theta_l \langle S_l^+ S_j^-\rangle + \frac{1}{2}\sin\theta_l \sin\theta_j \langle S_l^z\rangle \right] \right\}. \tag{3}$$

The excitation energy is given by the poles of the Green's function, which correspond to the eigenvalues of matrix A. In the case of a diagonal form, the excitation energy results in

$$\epsilon_n = 2\Omega_n \sin\theta_n + \sum_i J_{ni} \cos\theta_n \cos\theta_i \langle S_i^z\rangle + \frac{1}{2}\sum_i J_{ni} \sin\theta_n \sin\theta_i (\langle S_i^+ S_n^-\rangle + \langle S_i^- S_n^-\rangle), \tag{4}$$

where all quantities are defined in the rotated frame. In the same manner (see Ref. 38), we find the damping of the spin wave as

$$\gamma_n = \frac{\pi}{4}\sum_j J_{nj}^2(\cos\theta_n \cos\theta_j - 0.5 \sin\theta_n \sin\theta_j)^2 \bar{n}_j(1-\bar{n}_j) \times \delta(\epsilon_n - \epsilon_j + \epsilon_j - \epsilon_n), \quad (5)$$

where $\bar{n}_n = \langle S_n^- S_n^+ \rangle$ is the correlation function. It is calculated via the spectral theorem and by using the excitation energy in the random-phase approximation [Eq. (4)].

As stressed in Ref. 32, the local rotation angle θ_n is defined by $\langle S_n^{x'} \rangle = 0$. From here, we conclude

$$\tan\theta_n = \frac{2\Omega}{\sum_i J_{in}\langle S_n^z \rangle}.$$

This relation is valid both above ($\theta = \pi/2$) and below the phase transition temperature T_c. The relative polarization of the nth shell is given by

$$\sigma_n = \langle S_n^z \rangle = \frac{1}{2}\tanh\left(\frac{\epsilon_n}{2T}\right)\cos\theta_n. \quad (6)$$

The leading part of the transverse spin-wave energy ϵ_n, the soft-mode energy of the nth shell, is obtained from Eq. (4) after performing the backward rotation:

$$\epsilon_n = 2\Omega \sin\theta_n + \sum_i J_{in}\cos\theta_i \langle S_i^z \rangle. \quad (7)$$

All the microscopic entities calculated here will be analyzed in the following section.

III. NUMERICAL RESULTS AND DISCUSSION

In this section, we present the results for spherical FE nanoparticles. The graphs below are based on the numerical treatment of Eqs. (4)–(6), which yield the excitation energy, its damping, and the polarization. Typically, we use as the model parameters $J_b = 150$ K and $\Omega_b = 10$ K, which are characteristically for BTO.[39] First, let us offer the dependence of the polarization via the temperature, including surface and size effects. Due to the different numbers of next nearest neighbors or by the resulting strain and/or stress of especially small particles at the surface, the interaction constant at the surface J_s is, in general, different from the bulk value J_b.[39] In Fig. 2, the temperature dependence of the mean polarization is presented for different values of the surface interaction J_s and a fixed number of shells N.

The particle is made up of four shells as shown in Fig. 1(d). The variation of the coupling at the surface changes the polarization accordingly. A lowered surface interaction strength $J_s < J_b$ leads to a reduced polarization, which vanishes continuously at a lower critical temperature T_c. The opposite case $J_s > J_b$ yields a larger dipole moment and, consequently, an enhanced phase transition temperature T_c. This reflects the observation that both the bulk and the surface couplings contribute to the ordering of the pseudospins. The phase transition is a pronounced second order one. In this approach, a variation of J is also possible through strain. This effect is included implicitly. An *ab initio* study of the polarization as a function of temperature is given in Ref. 40.

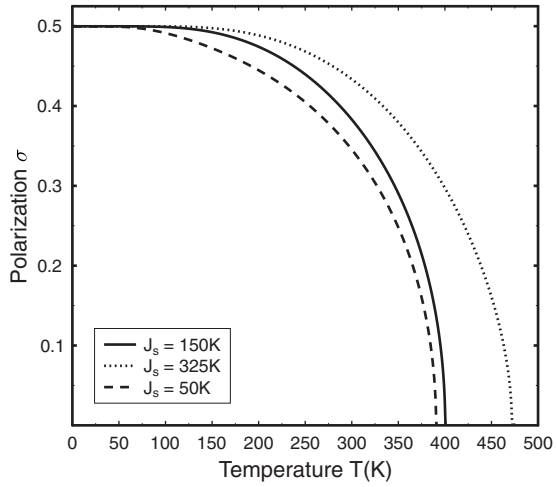

FIG. 2. Temperature dependence of the averaged polarization σ with $J_b = 150$ K and $N = 4$ for different surface couplings: $J_s = J_b$ (solid curve), $J_s = 325$ K (dotted curve), and $J_s = 50$ K (dashed curve).

For a more detailed observation, the shell resolved polarization σ_n is given in Figs. 3 and 4 for a particle with eight shells ($N = 8$). The index n denotes the position in the particle; e.g., $n = 8$ represents the surface shell. The reduction of the local polarization σ_n depending on the position within the particle is clearly visible. The behavior for weaker surface coupling is opposite to that for stronger surface coupling. The smaller the strength J_s compared to the bulk value J_b, the faster is the decrease of the polarization in the outer shells. A higher J_s provides smaller values in the inner shells. This reflects the importance of the inclusion of surface effects. The case $J_s < J_b$ (see Fig. 3) could explain the decrease of the polarization and the phase transition temperature in small particles of BTO[11,12] and PTO,[17,41] while the second case (cf. Fig. 4) is responsible for the increase of the polarization and T_c in small KDP particles[42] and KNO_3 thin films.[43] Because we are mainly interested in the properties of

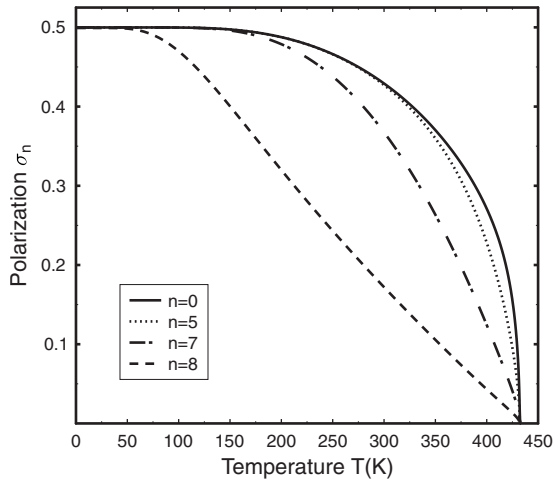

FIG. 3. Temperature dependence of the shell resolved polarization σ_n for different shells n with $J_s < J_b$, where $J_b = 150$ K, $J_s = 50$ K, and $N = 8$.

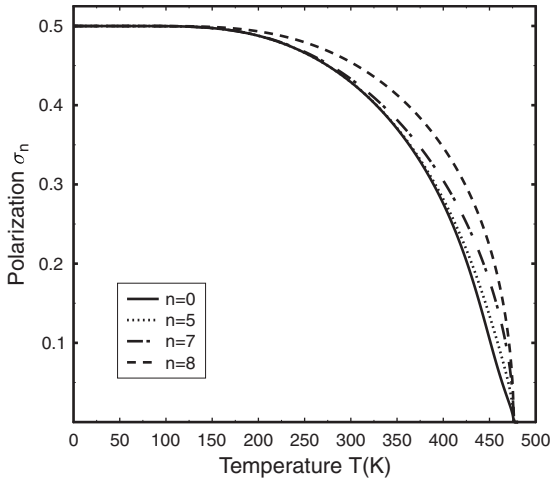

FIG. 4. Temperature dependence of the shell resolved polarization σ_n for different shells n with $J_s > J_b$, where $J_b = 150$ K, $J_s = 325$ K, and $N = 8$.

BTO-type FE small particles, the forthcoming investigations concentrate on the case $J_s < J_b$.

As already pointed out in the Introduction, there is a long-standing debate how physical properties like the polarization or the critical temperature are affected by the size of the system, especially in the nanometer scale. Therefore, we have calculated within our microscopic model the dependence of polarization on size. The result is depicted in Fig. 5. In the present case, the size is controlled by the number of shells N. Obviously, the polarization is enhanced with increasing particle size. Summarizing all the data, the phase transition temperature versus the number of shells is shown in Fig. 6. The FE particles exhibit a fast increase of T_c with an ascending number of shells. In the limit of very large numbers N, the critical temperature approaches nearly the constant bulk value. The result is in qualitative agreement with the experimental data of small particles composed of BTO[12] and PTO.[17,41] However, the chosen set of parameters

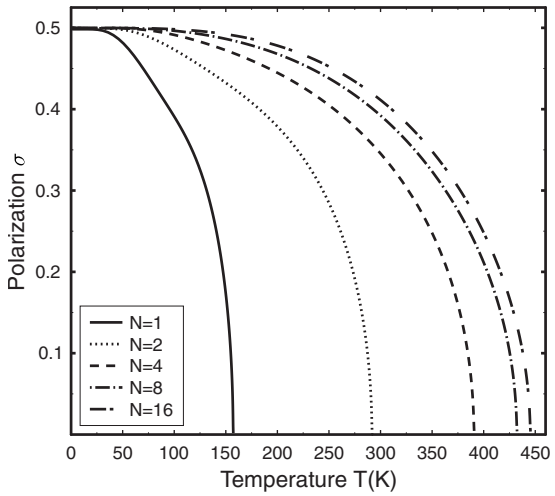

FIG. 5. Temperature dependence of the polarization σ for $J_s < J_b$ with $J_b = 150$ K, $J_s = 50$ K, and different numbers of shells N.

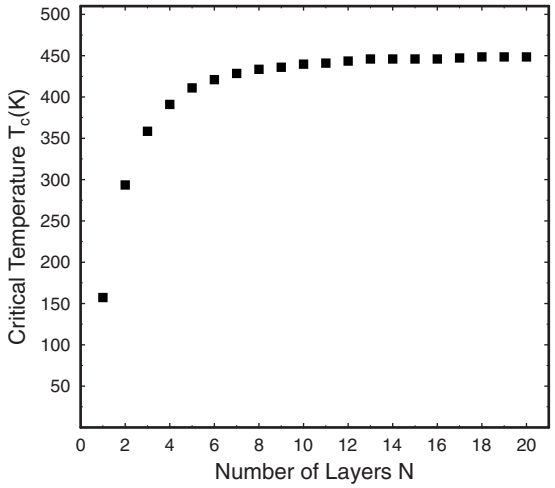

FIG. 6. Critical temperature T_c depending on the number of shells N with $J_b = 150$ K and $J_s = 50$ K.

does not lead to an indication of a pronounced critical size effect as argued before. This point deserves a more refined procedure.

Apart from macroscopic quantities such as the polarization, the method allows us also to find microscopic features of the nanoparticles such as the energy of the elementary excitations [cf. Eq. (4)], and its damping [see Eq. (5)]. In Fig. 7, the temperature dependence of the excitation energy is plotted for a different number of shells when the relation $J_s < J_b$ is fulfilled. One observes a lowering of the excitation energy with increasing temperature. The larger the particles, the higher are the energies. The nanoparticle shows a typical soft-mode behavior as already observed in the bulk material. Apparently, the excitation energy is shifted to smaller values in comparison to the bulk material when the number of shells decreases. The result implies a lowering of the force constant in the small particle, which was observed for PTO

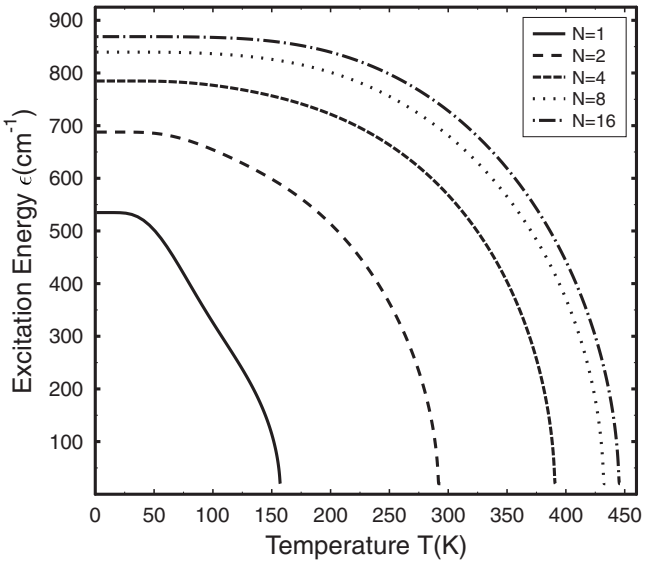

FIG. 7. Temperature dependence of the excitation energy for different numbers of shells N with $J_b = 150$ K and $J_s = 50$ K.

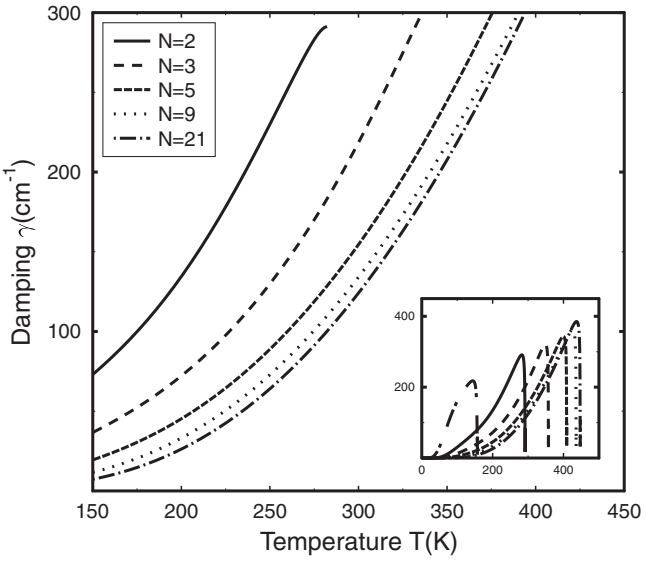

FIG. 8. Temperature dependence of the damping of the excitation energy for different numbers of shells N with $J_b=150$ K and $J_s=50$ K.

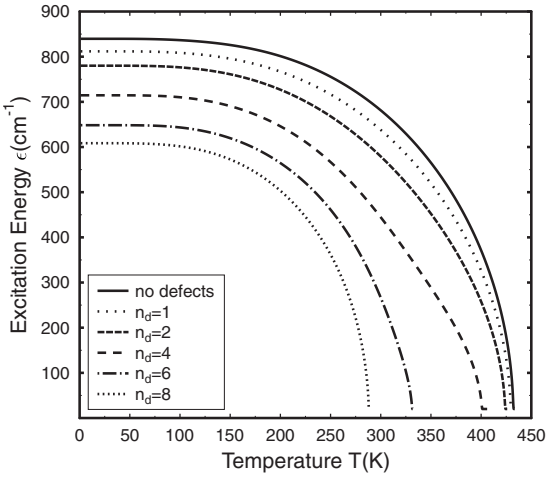

FIG. 9. Temperature dependence of the excitation energy for $J_b>J_s>J_d$ with different defect shells: $J_b=150$ K, $J_s=50$ K, $J_d=25$ K, and $N=8$.

particles.[16,17,44] Consequently, this leads to the decrease of the phase transition temperature between the tetragonal and cubic phases.

Due to higher order interactions between the constituents and/or due to the scattering at defects or due to the inclusion of phonon degrees of freedom, the elementary excitation can be damped. Such a damping could be manifested in a finite lifetime of the excitation. Here, we have calculated the damping according to Eq. (5). In Fig. 8, the temperature dependence of the damping is plotted. When the particle size is lowered, the damping increases. At low temperatures, the damping is extremely small, clearly even smaller than the excitation which is underdamped accordingly. In approaching the critical temperature T_c, the damping increases strongly but remains finite (see Fig. 8). This behavior is in contrast to the behavior of the bulk material, where the linewidth of the soft mode diverges at the ferroelectric-to-paraelectric transition in PTO.[45] In the vicinity of T_c, the soft mode becomes overdamped. Such a behavior is, however, in agreement with experimental data for PTO,[16,44] BTO,[21] and SBT[20] particles. The enhanced damping in small nanoparticles, obtained here, could be an explanation for the broadened peak, observed in the dielectric constant of PTO particles[41] and $(Ba,Sr)TiO_3$ thin films.[46,47] A broadened dielectric anomaly leads also to a smearing out of the critical regime. The inset shows the overall development of the damping. Very close to the critical point, a sudden decrease was observed, which is only plotted in the inset for the sake of completeness. Because in our Green's function method fluctuation effects, predominantly occurring in the vicinity of the phase transition, are slightly suppressed, the results presented should be considered as an extrapolation to illustrate the behavior near T_c. A more refined calculation of the damping near T_c will be given elsewhere.[48]

Experiments show a clear influence of impurities or defects on physical properties. For this reason, let us incorporate also defect configurations into the model. The simplest way is to assume that the interaction strength J varies in the case of defects. The defect coupling is denoted as J_d. Physically, this variation of the coupling parameter can be originated from the appearance of local stress, by the substitution of ions with different radii and, consequently, different distances between them (smaller radii correspond to larger distances), and by localized vacancies. The excitation energy as well as its damping should depend on the defect concentration. The temperature dependence of the energy of the elementary excitations for different numbers of defect shells, denoted as n_d, is shown in Fig. 9. For instance, $n_d=4$ means all up to the fourth shell are defect ones. In Fig. 9, the bulk coupling is stronger than the defect coupling, i.e., $J_b>J_s>J_d$. The excitation energy depends on both the number of defects n_d and the corresponding coupling J_d. For an enhanced defect concentration, ϵ is reduced. In the case of $J_s<J_b<J_d$, the opposite behavior of the excitation energy is observed. The excitation energy is increased for all temperatures up to the critical point. For the first case, we have also analyzed the behavior of the damping of excitations, which is depicted in Fig. 10. There is experimental evidence that for La-doped nanocrystalline PTO[49] and for Er- and La-substituted PTO thin films,[50] the soft-mode frequency is lowered and the Raman peak width is broadened in comparison to the undoped specimen. Let us emphasize that our results reveal that different mechanisms such as surfaces, stress, and defects contribute additively to the damping coefficient. The damping is always enhanced in comparison to the bulk and to materials without defects.

IV. CONCLUSION

Ferroelectrics are widely used in many applications that require sizes down to the nanometer range. Although the main challenge is to fabricate structures in the nano region, there is also an increasing interest in modeling ferroelectric nanoparticles. Due to the fact that the behavior is obviously

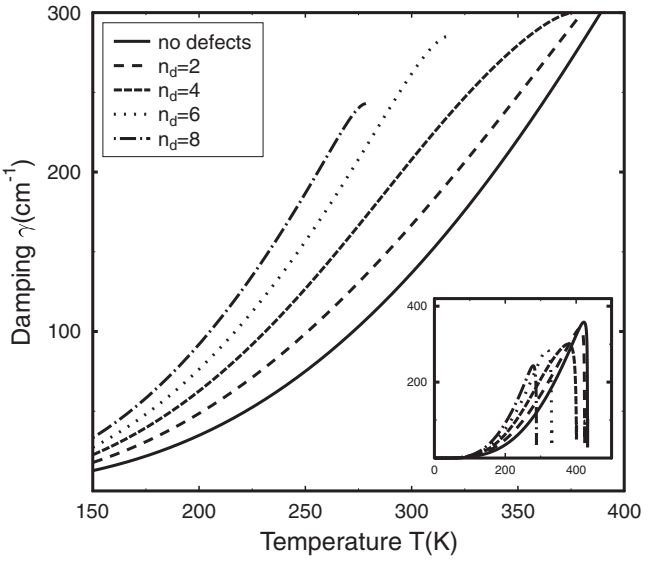

FIG. 10. Temperature dependence of the damping for $J_b > J_s > J_d$ with different defect shells: $J_b = 150$ K, $J_s = 50$ K, $J_d = 25$ K, and $N = 8$.

determined by the microscopic interaction between the constituents, it seems natural to consider models on that scale instead of the mesoscopic or macroscopic ones. In the present paper, we have calculated within such a microscopic model those macroscopic quantities such as the polarization and, additionally, dynamic features such as the excitation energy and its damping. To that aim, one of the standard models for describing bulk properties of ferroelectric materials, the Ising model in a transverse field, is modified in such a manner as to be able to find out the quantities mentioned before. This approach and the method of Green's functions in real space yield the polarization and associated dynamic properties of nanoparticles. As the simplest case, spherical particles composed of different shells were analyzed. This number corresponds directly to the size of the particle. The small size of the materials requires the inclusion of both bulk and surface interactions. Furthermore, in case of the appearance of defects, there occurs an additional coupling strength. Taking into account the microscopic parameters (direct coupling and transverse field), the temperature and size dependence of the polarization as well as the excitation energy and its damping were obtained. Whereas the excitation energy decreases, the damping increases strongly with decreasing particle size. Furthermore, damping of the quasi-soft-mode in nanoparticles is significantly larger than that in bulk crystals. The results obtained are in agreement with the experimental data for BTO and PTO small particles.

ACKNOWLEDGMENTS

Two of us (T.M. and J.M.W.) acknowledge support by the International Max Planck Research School for Science and Technology of Nanostructures in Halle, Germany. This work is further supported by the SFB 418.

*thomas.michael@physik.uni-halle.de
†steffen.trimper@physik.uni-halle.de
‡julia@phys.uni-sofia.bg

[1] J. Jacard, W. Kaenzig, and M. Peter, Helv. Phys. Acta **26**, 521 (1953).
[2] M. Anliker, H. R. Brugger, and W. Kaenzig, Helv. Phys. Acta **27**, 99 (1954).
[3] M. Dawber, K. M. Rabe, and J. F. Scott, Rev. Mod. Phys. **77**, 1083 (2005).
[4] P. Ghosez and J. Junquera, *Handbook of Theoretical and Computational Nanotechnology* (ASP, Stevenson Ranch, CA, 2006), Vol. 7.
[5] W. Kohn, Rev. Mod. Phys. **71**, 1253 (1999).
[6] K. M. Rabe and J. D. Joannopoulos, Phys. Rev. Lett. **59**, 570 (1987).
[7] W. Zhong, D. Vanderbilt, and K. M. Rabe, Phys. Rev. Lett. **73**, 1861 (1994).
[8] S. Tinte, M. G. Stachiotti, M. Sepliarsky, R. L. Migoni, and C. O. Rogriguez, J. Phys.: Condens. Matter **11**, 9679 (1999).
[9] I. Grinberg, V. R. Cooper, and A. M. Rappe, Nature (London) **419**, 909 (2002).
[10] M. G. Stachiotti, Appl. Phys. Lett. **84**, 251 (2004).
[11] S. Schlag and H. F. Eicke, Solid State Commun. **91**, 883 (1994).
[12] T. Ohno, D. Suzuki, K. Isjikawa, M. Horiuchi, T. Matsuda, and H. Suzuki, Ferroelectrics **337**, 25 (2006).
[13] T. Hoshina, H. Kakemoto, T. Tsurumi, and S. Wada, J. Appl. Phys. **99**, 054311 (2006).
[14] M. H. Frey and D. A. Payne, Appl. Phys. Lett. **63**, 2753 (1993).
[15] W. L. Zhong, P. L. Zhang, Y. G. Wang, and T. L. Ren, Ferroelectrics **160**, 55 (1994).
[16] K. Ishikawa, K. Yoshikawa, and N. Okada, Phys. Rev. B **37**, 5852 (1988).
[17] W. L. Zhong, B. Jiang, P. L. Zhang, J. M. Ma, H. Chen, Z. H. Yang, and L. Li, J. Phys.: Condens. Matter **5**, 2619 (1993).
[18] B. D. Qu, B. Jiang, Y. G. Wang, P. L. Zhang, and W. L. Zhong, Chin. Phys. Lett. **11**, 514 (1994).
[19] V. Nagarajan, T. Zhao, J. Ouyang, R. Ramesh, W. Tain, X. Pan, D. S. Kim, C. B. Eom, H. Kohlstedt, and R. Waser, Appl. Phys. Lett. **84**, 5225 (2004).
[20] T. Yu, Z. X. Shen, W. S. Toh, J. M. Xue, and J. Wang, J. Appl. Phys. **94**, 618 (2003).
[21] S. Wada, T. Hoshina, H. Yasuno, M. Ohishi, H. Kakemoto, T. Tsurumi, and M. Yashima, in *Advances in Electronic Ceramic Materials*, edited by D. Zhu and W. M. Kriven (Wiley, New York, 2005), Vol. 26, p. 89.
[22] A. Jana, T. K. Kundu, S. K. Pradhan, and D. Chakravorty, J. Appl. Phys. **97**, 044311 (2005).
[23] W. L. Zhong, Y. G. Wang, P. L. Zhang, and B. D. Qu, Phys. Rev. B **50**, 698 (1994).
[24] Y. G. Wang, W. L. Zhong, and P. L. Zhang, Solid State Commun. **90**, 329 (1994).
[25] C. L. Wang and S. R. P. Smith, J. Phys.: Condens. Matter **7**, 7163

(1995).
[26] C. L. Wang, S. R. P. Smith, and D. R. Tilley, Ferroelectrics **186**, 33 (1996).
[27] L. Baudry, Ferroelectrics **333**, 27 (2006).
[28] A. N. Morozovska, E. A. Eliseev, and M. D. Glinchuk, Phys. Rev. B **73**, 214106 (2006).
[29] Y. G. Wang, W. L. Zhong, and P. L. Zhang, Solid State Commun. **101**, 807 (1997).
[30] C. L. Wang, Y. Xin, X. S. Wang, and W. L. Zhong, Phys. Rev. B **62**, 11423 (2000).
[31] W. L. Zhong, J. Korean Phys. Soc. **32**, S265 (1998).
[32] Th. Michael, S. Trimper, and J. M. Wesselinowa, Phys. Rev. B **74**, 214113 (2006).
[33] R. Blinc and B. Žekš, *Soft Modes in Ferroelectrics and Antiferroelectrics* (North-Holland, Amsterdam, 1974).
[34] H. X. Cao and Z. Y. Li, J. Phys.: Condens. Matter **15**, 6301 (2003).
[35] Q. Zhang, F. Chen, N. Kioussis, S. G. Demos, and H. B. Radousky, Phys. Rev. B **65**, 024108 (2001).
[36] S. Koval, J. Kohanoff, R. L. Migoni, and E. Tosatti, Phys. Rev. Lett. **89**, 187602 (2002).
[37] G. F. Reiter, J. Mayers, and P. Platzman, Phys. Rev. Lett. **89**, 135505 (2002).
[38] Yu. Tserkovnikov, Theor. Math. Phys. **7**, 250 (1971).
[39] J. M. Wesselinowa, Phys. Status Solidi B **223**, 737 (2001).
[40] D. A. Tenne *et al.*, Science **313**, 1614 (2006).
[41] S. Chattopadhyay, P. Ayyub, V. R. Palkar, and M. Multani, Phys. Rev. B **52**, 13177 (1995).
[42] E. V. Colla, A. V. Fokin, and Yu. A. Kumzerov, Solid State Commun. **103**, 127 (1997).
[43] J. F. Scott, M.-S. Zhang, R. B. Godfrey, C. Araujo, and L. McMillan, Phys. Rev. B **35**, 4044 (1987).
[44] D. Fu, H. Suzuki, and K. Ishikawa, Phys. Rev. B **62**, 3125 (2000).
[45] G. Burns and B. A. Scott, Phys. Rev. Lett. **25**, 167 (1970).
[46] C. B. Parker, J.-P. Maria, and A. I. Kingon, Appl. Phys. Lett. **81**, 340 (2002).
[47] D. A. Tenne, A. M. Clark, A. R. James, K. Chen, and X. X. Xi, Appl. Phys. Lett. **79**, 3836 (2001).
[48] S. Trimper, T. Michael, and J. Wesselinowa (unpublished).
[49] J. Meng, G. Zou, J. Li, Q. Cui, X. Wang, Z. Wang, and M. Zhao, Solid State Commun. **90**, 643 (1994).
[50] S. Yakovlev, C.-H. Solterbeck, E. Skou, and M. Es-Souni, Appl. Phys. A: Mater. Sci. Process. **82**, 727 (2006).